



Geophysical Research Letters

RESEARCH LETTER

10.1029/2018GL081302

Key Points:

- Solar heating of optically thick canopy clouds lifts outflow in the afternoon
- This afternoon outflow lifting explains the afternoon peak in cloud top height
- The diurnal variation of insolation does not impact the timing of spontaneous cyclogenesis in RCE

Supporting Information:

- Supporting Information S1
- Figure S1
- Figure S2
- Movie S1

Correspondence to:

J. H. Ruppert,
james.ruppert@psu.edu

Citation:

Ruppert, J. H., & O'Neill, M. E. (2019). Diurnal cloud and circulation changes in simulated tropical cyclones. *Geophysical Research Letters*, 46, 502–511. <https://doi.org/10.1029/2018GL081302>

Received 12 NOV 2018

Accepted 28 DEC 2018

Accepted article online 4 JAN 2019

Published online 11 JAN 2019

Diurnal Cloud and Circulation Changes in Simulated Tropical Cyclones

James H. Ruppert Jr.^{1,2} and Morgan E. O'Neill³

¹Max Planck Institute for Meteorology, Hamburg, Germany, ²Now at the Department of Meteorology and Atmospheric Science, Pennsylvania State University, University Park, PA, USA, ³Department of Earth System Science, Stanford University, Stanford, CA, USA

Abstract Observations of the diurnal cycle in tropical cyclones (TCs) systematically indicate a ~12-hr offset between peak rainfall rate and the maximum height of anvil clouds in the TC cloud canopy. This phasing conflicts with archetypal models of organized deep convection, which suggest a tight coupling between rainfall, vertical cloud growth, and anvil clouds. We show that this phasing owes to the bimodal diurnal evolution of the transverse circulation, which peaks nocturnally from low–midlevels, and during daytime in the upper troposphere. The bottom-heavy nocturnal circulation state is driven by latent heating from nocturnally invigorated deep convection, while the top-heavy daytime state is the thermally direct circulation response to strong shortwave-cloud warming in the optically thick TC cloud canopy. This daytime upper-level circulation response manifests in a lifting of the maximum height of the TC outflow and, in turn, a lifting and invigoration of the upper-level anvil clouds of the TC cloud canopy.

Plain Language Summary We typically expect the rainfall, deeply growing thunderstorm clouds, and outward-spreading anvil clouds in tropical cyclones (e.g., hurricanes) to closely coincide in time—that is, when rainfall peaks, we expect deep clouds to be vigorously growing, and anvil clouds in the upper-level cloud canopy to be spreading outward and at their greatest height. Previous observational studies, however, indicate that in the 24-hr diurnal cycle, anvil clouds behave distinctly from the deep thunderstorm clouds that produce the rain: while rainfall and deep clouds peak overnight, the height and spreading of the anvil clouds peaks during the day. This study indicates that this distinct behavior of anvil clouds owes to the interaction between solar radiation and ice clouds. Namely, the abundant ice crystals in anvil clouds absorb much of the incoming solar radiation, leading to strong warming there. This daytime warming, in turn, enhances the upward motion at the height of these anvil clouds, causing the storm's upper-level outflow to lift. The lifting of outflow promotes the anvil clouds to lift and spread. This lifting of anvil clouds in the outflow maximizes in the early afternoon, even though rainfall is suppressed during daylight hours.

1. Introduction

The diurnal cycle of 24-hr period is the largest mode of rainfall variability in the tropics (Kikuchi & Wang, 2008). Mounting evidence indicates that diurnal variability in clouds and convection affects weather and climate at longer time scales through nonlinear rectification (Bergman & Salby, 1997; Cronin et al., 2015; Ruppert, 2016; Ruppert & Johnson, 2016). Improving our understanding of this mode, and its efficacy in climate models, should therefore improve our predictions of global climate (Dirmeyer et al., 2012; Neale & Slingo, 2003). On subdaily time scales, the diurnal cycle yields inherent predictability that can be invaluable in operational settings. Take the case of a strong landfalling tropical cyclone (TC), wherein extreme rainfall is often the most catastrophic impact (e.g., Blake & Zelinsky, 2018; Hurricane Harvey, 2017): exploiting the predictability linked to the diurnal cycle can potentially save lives and minimize economic loss. Yet doing so requires that we properly understand and model it.

A predominant nocturnal or early-morning rainfall peak has been noted in many forms of organized deep convection over the tropical oceans, including both TCs (Bowman & Fowler, 2015; Dunion et al., 2014) and the intertropical convergence zone (ITCZ) (Ciesielski et al., 2018). The underlying cause for this nocturnal peak has been deliberated for several decades (Chen & Houze, 1997; Dai, 2001; Gray & Jacobson, 1977; Kraus, 1963; Randall et al., 1991; Yang & Smith, 2006). Growing evidence points toward cloud-radiation

interaction as the key cause. While longwave emission perpetually acts to cool cloud tops, direct shortwave absorption warms cloud tops during daytime (Webster & Stephens, 1980). The resulting diurnal variation of static stability suppresses convection during daytime and invigorates it overnight (Randall et al., 1991; Xu & Randall, 1995). This effect is augmented by radiatively driven circulation changes: as low-level radiative cooling nocturnally increases in the cloud-free surroundings of a large convective system, low-level convergence into the system is enhanced (Gray & Jacobson, 1977; Nicholls, 2015; Ruppert & Hohenegger, 2018).

The nocturnal–early-morning peak in rainfall in TCs would imply that the anvil clouds comprising the upper-level TC cloud canopy would also peak at this time. Yet satellite observations systematically indicate an afternoon peak in the coverage and maximum height of these canopy clouds, that is, essentially in opposing phase with rainfall (Bowman & Fowler, 2015; Dunion et al., 2014; Kossin, 2002; Melhauser & Zhang, 2014; Leppert & Cecil, 2016; Wu & Ruan, 2016). This offset phasing conflicts with archetypal models of organized deep convection, wherein rainfall, deep cumulonimbus cloud growth, and anvil cloud spreading are tightly coupled (Mapes et al., 2006; Yuan & Houze, 2010; Zipser, 1969). Furthermore, we may naively assume that the time-mean transverse circulation pattern—low-level inflow and upper-level outflow—is nocturnally amplified in connection with rainfall. The afternoon peak of anvil clouds, however, implies a more complex diurnal evolution. Such complexity, if present, would have implications for our basic understanding of TCs. Furthermore, if such complexity manifests in diurnal changes to the transport of moisture or dry air into the convective core (e.g., ventilation), this process may also have important implications for TC prediction (Kimball, 2006; Tang & Emanuel, 2010).

The diurnal cycle of TCs is investigated here through idealized cloud-permitting numerical simulations. A miniature ensemble is conducted wherein top-of-atmosphere (TOA) insolation either varies diurnally or is fixed at its daily mean. This simulation set enables us to assess the nonlinear impact of the diurnal cycle on the timing of tropical cyclogenesis. While prior studies have examined the distinct effects of including or excluding shortwave heating on TCs (e.g., Melhauser & Zhang, 2014; Tang & Zhang, 2016), no study allowing spontaneous cyclogenesis has performed tests with constant mean TOA insolation as a control. A simulation with diurnally varying radiation is then examined in detail to investigate the response of the transverse or secondary circulation to diurnally varying radiative-cloud warming. We show that understanding the paradoxical diurnal behavior of TC canopy clouds (or anvil clouds), as described above, requires understanding the circulation response to upper-level shortwave-cloud warming.

2. Study Methods

An idealized modeling approach is taken here to isolate processes of interest. We conduct cloud-permitting simulations in the rotating radiative-convective equilibrium (RCE) framework using an f -plane corresponding to 20° N, similar to many prior studies (e.g., Davis, 2015; Khairoutdinov & Emanuel, 2013; Nolan et al., 2007; O'Neill et al., 2017; Wing et al., 2016). In this framework, no background wind or initial disturbance is imposed, and cyclogenesis occurs spontaneously through convective self-aggregation (Bretherton et al., 2005): initially randomly distributed deep-convective elements cluster as a cyclone forms and intensifies, due to a concert of feedbacks between clouds, circulation, surface fluxes, and longwave radiation (Wing et al., 2016).

The RCE simulations are conducted using the large-eddy model framework of the icosahedral nonhydrostatic model (ICON-LEM) (Dipankar et al., 2015), which employs a Smagorinsky-type turbulence parameterization. ICON-LEM was employed similarly in nonrotating RCE by Ruppert and Hohenegger (2018). The horizontal domain is a doubly periodic 2,000 × 2,000-km grid discretized using a Delauney mesh of triangular cells of edge-length 3 km (Cartesian-equivalent grid spacing of ~2 km). A stretched vertical grid of 75 levels is employed, with spacing of 50 m near the surface and 500 m near model top at 27 km, and a sponge layer from 19 km and up to absorb gravity waves. The spacing of ~400 m in the upper troposphere is inadequate to resolve thin (e.g., cirrus) clouds, although it is adequate for resolving thick (i.e., optically thick) anvil clouds. The physics parameterizations include a two-moment microphysics scheme (Seifert & Beheng, 2006), fully interactive Rapid Radiative Transfer Model (RRTM) radiation (Clough et al., 2005; Iacono et al., 2008; Mlawer et al., 1997), and interactive surface fluxes. Sea surface temperature is fixed to 301 K. Radiation is calculated every 300 s, with diurnally varying, horizontally invariant zenith angle corresponding to equinox at 19.45° N. Although insolation is fixed implying a fixed Julian day, the diurnal cycle is likely amplified or suppressed under summertime or wintertime insolation.

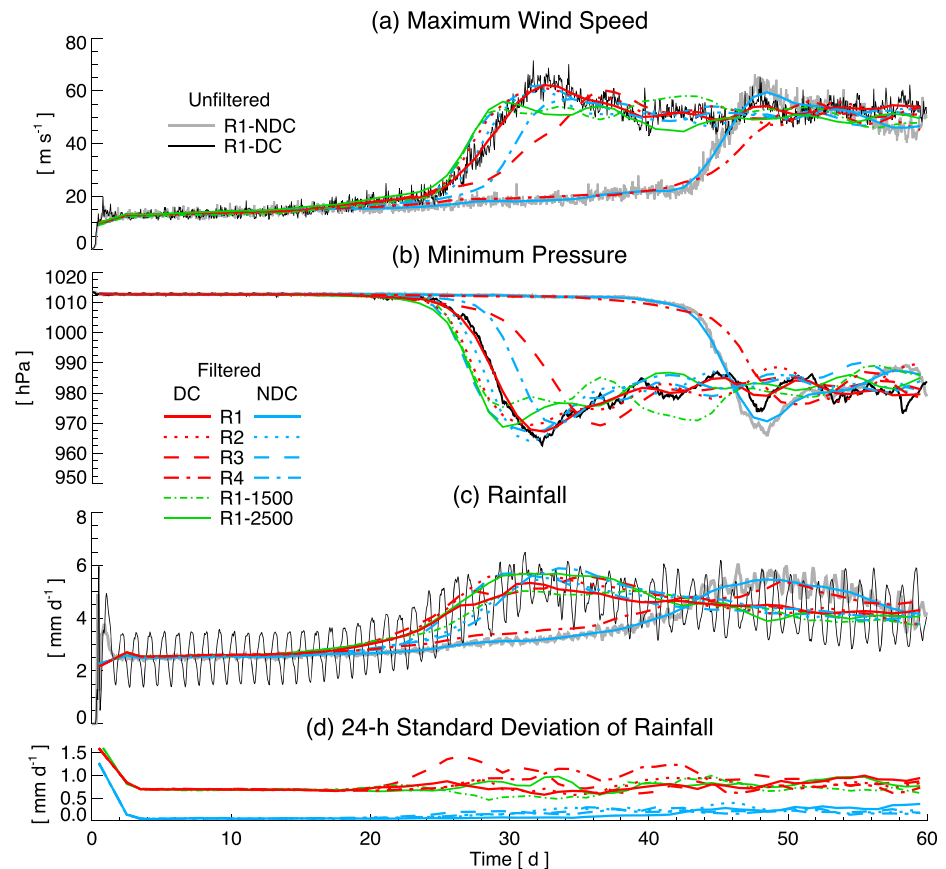


Figure 1. Time series for each of the simulations, filtered (red and blue) using 3-day boxcar smoothing, with (a) maximum wind speed at the lowest model level (25 m), (b) minimum surface pressure, (c) domain-mean rainfall, and (d) 24-hr standard deviation of rainfall. The unfiltered time series for R1-NDC (gray) and R1-DC (black) are shown (a–c) as examples of the full spectrum of variability.

A miniature ensemble is conducted to assess the impact of diurnal forcing relative to stochasticity: four simulations where TOA insolation varies diurnally (R^* -DC, where the asterisk stands in for 1–4), and four with TOA insolation fixed to the daily mean (R^* -NDC). Each simulation is initialized from the same homogeneous RCE initial state: the time- and domain-averaged state from 70–90 days of a simulation conducted using the above-described physics but on a small domain of 100×100 km, wherein aggregation does not occur. Random noise of $\leq |0.3|$ K and $\leq |0.1|$ m/s is added to the initial virtual temperature and vertical motion w fields in the lowest three model levels of each simulation to initiate convection, with the noise changed for each set R^* (similar to Wing et al., 2016). Two additional experiments were conducted to assess the impact of domain size on the results: R1-1500 and R1-2500, which are identical to R1-DC except with model domains of 1,500- and 2,500-km edge length. All analysis is conducted using hourly model output. With the exception of the time series in Figure 1, all variables are azimuthally averaged to examine the bulk, axisymmetric properties of the diurnal cycle.

3. Results

3.1. Simulation Overview

The evolution of each simulation is presented through basic measures of storm intensity in Figure 1, filtered to exemplify day-to-day changes. (A three-dimensional depiction of this evolution is exemplified through maps of column water vapor and ice water path (IWP), provided for R1-DC in supporting information Figure S1.) Cyclogenesis is indicated by the sudden step increase in wind speed and decrease in pressure, beginning no sooner than 20 days (Figures 1a and 1b). Each simulation is characterized by coinciding maxima in wind speed and rainfall and minima in pressure after a primary period of TC intensification, followed by slight reductions in intensity by these measures (Figure 1a–1c). The simulations then approach pressure and

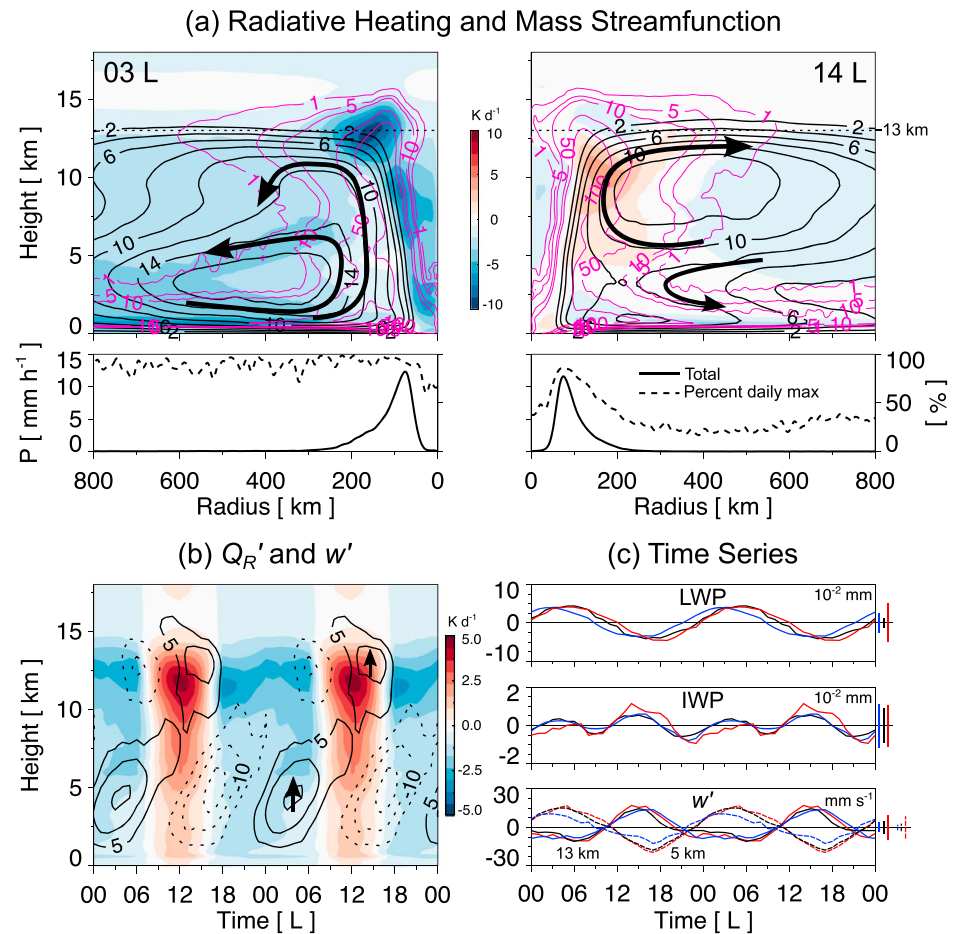


Figure 2. Diurnal cycle in the 35–60-day composite of the simulation R1-DC. (a) Azimuthally averaged cross sections for (left) 03 and (right) 14 L: (upper) radiative heating Q_R (shading; K/day), specific cloud liquid + ice content q_t (magenta contours; mg/kg), and streamfunction ψ (black contours; 10^8 kg/s); and (lower) precipitation total (solid; mm/hr) and percentage of the daily maximum (dashed). (b) Q'_R (daily mean removed; shading) and vertical motion w' (daily mean removed; contours; mm/s) averaged over radii 100–300 km. (c) Time series of (upper) cloud LWP and (center) cloud IWP (daily means removed), (lower) w' at (dashed) 5 and (solid) 13 km in the vertical, and error bars (vertical lines at right ordinate) averaged over 100–300 km. (c) includes simulations R1-DC (black), 1500KM (blue), and 2500KM (red). LWP = liquid water path; IWP = ice water path.

wind values of 980 hPa and ~ 50 m/s (category 3 on the Saffir-Simpson scale). Such wind speeds typically correspond to storms of 960-hPa minimum pressure in nature (Chavas et al., 2017). We do not understand the origin of this discrepancy. Nevertheless, the diurnal cycle in these simulations is highly consistent with TCs in nature, as described in the next section.

While each simulation eventually approaches similar equilibrium values of wind speed and pressure (by 50 days), there is a large range of ~ 21 days between the earliest and latest day of genesis (e.g., R1-NDC and R4-DC). The spread among simulations is bimodal, with genesis between 25 and 30 d in eight simulations and around 44 d in the remaining two. Surprisingly, the varied initial conditions appear to explain these differences, while including or excluding the diurnal variation of insolation does not bias the four-member spread. Therefore, the impact of the diurnal cycle on the timing of tropical cyclogenesis is negligible in this simulation set. Next, we study one of the diurnally varying simulations to investigate the nature of diurnal cloud-radiation interaction and its influence on circulation in a mature TC.

3.2. The Diurnal Cycle

The unfiltered hourly time series for R1-NDC and R1-DC exemplify the full spectrum of variability in the simulated TCs (Figures 1a–1c). Only rainfall exhibits a clear, pronounced diurnal cycle among these variables. The diurnal amplitude is approximately 25% of the (postgenesis) mean rain rate, with a range of

~2 mm/day. While rainfall in R1-NDC exhibits high-frequency variability, which amplifies after TC intensification, this variability is far weaker than the diurnal cycle in R1-DC. The same can be said for each of the four simulation sets, as demonstrated by 24-hr standard deviation (Figure 1d). This implies that the diurnal cycle can be readily examined through time compositing without filtering.

The remainder of the analysis focuses on the diurnal cycle in the representative simulation R1-DC. The period from 35–60 days covers the quasi-steady state period of the TC following primary intensification. Diurnal composites are generated by time-averaging over this 25-day period as a function of local solar time (L). Different time subsets were also examined, with qualitatively similar results (not shown).

Azimuthally averaged cross sections of mass streamfunction, ψ exemplify the two distinct transverse circulation states of night and day (Figure 2a). (See also 24-hr composite animation provided as supporting information Movie S1.) While the strong, deep ascending motion within the sloped eyewall persists through the diurnal cycle, the circulation beyond the eyewall exhibits pronounced diurnal changes. The nocturnal flow at 03 L exhibits a bottom-heavy shape, with enhanced inflow in the lowest 3 km, low–midlevel ascending motion at radii ~100–300 km, and a secondary outflow (secondary to that of the upper troposphere) from around 4–8 km vertically, which descends with increasing radius. The circulation state at 14 L is characterized by greatly reduced inflow in the lower free troposphere and an inflow in place of the nighttime midlevel outflow. The diurnal anomalies of radial wind associated with these inflow-outflow reversals are ~4 m/s (not shown). The daytime midlevel inflow and the upper-tropospheric outflow comprise an apparent instantaneous circulation cell (i.e., from ~5–13 km), although it is unlikely that a parcel completes a full circuit before the circulation phase changes to the nighttime state. The subsiding branch of this daytime upper-level cell is beyond a radius of 500 km, while at 03 L, upper-level subsidence begins around 400 km. Qualitatively similar diurnal circulation changes were found in organized deep convection in nonrotating RCE by Ruppert and Hohenegger (2018) and in axisymmetric TC simulations by Navarro and Hakim (2016).

The very bottom-heavy shape of the nighttime circulation state, with enhanced outflow at midlevels, is associated with enhanced column-integrated import of water vapor (or air of high moist static energy) into the storm core. This is consistent with enhanced deep convection and rainfall (Figure 2a; cf. also Figure 3d). The midlevel inflow at 14 L, in contrast, drives greater import of dry air (low moist static energy), suppressed convection, and a greater proportion of stratiform rainfall (Houze, 1997; Zipser, 1977). The diurnal variation of column-integrated moisture convergence in the storm core (radii from 100–300 km) supports these inferences (not shown). This diurnal cycle indicates that the TC is diurnally most susceptible to the detrimental effects of dry-air entrainment, or ventilation, around midday–afternoon (Kimball, 2006; Tang & Emanuel, 2010).

The diurnal evolution of circulation is depicted in Figure 2b through a time-height series of w' (w with the daily mean removed), averaged over 100–300 km. This radial range captures nearly the entire radial region characterized by mean upward motion and is henceforth referred to simply as the TC inner core (Figure 2a; results are qualitatively insensitive to modest changes in the bounds of this range). Two distinct diurnal peaks are apparent, which are of the same order of those described by Navarro and Hakim (2016) and Ruppert and Hohenegger (2018): a nocturnal peak centered at ~5 km vertically and an early-afternoon peak centered at ~13 km. These peaks correspond to the bottom-heavy nighttime and top-heavy daytime ψ regimes in Figure 2a. The nighttime peak extends from the boundary layer to ~8 km, reflecting enhanced deep convection during this time period. The magnitude decrease of w' with height from 5–8 km indicates enhanced divergence in this layer, consistent with the midlevel outflow apparent in ψ at 03 L (Figure 2a).

The early-afternoon w' maximum is situated at the very top of the primary outflow (~13 km; Figures 2a and 2b). Since this w' signal is of the same sign as time-mean vertical motion in this region, this maximum may be interpreted as a lifting of the top of the secondary circulation or the outflow. Comparison of the height of the uppermost ψ contours between 03 and 14 L corroborates this argument and, furthermore, indicates that this circulation lifting extends out to at least 600 km in radius. This upper-level w' maximum is characterized by a distinct outward radial progression with time in the afternoon, as is explored in detail later.

The nighttime circulation state is associated with a pronounced upper-level peak in radiative cooling ($Q_R < 0$) of ~10 K/day in the TC inner core (Figure 2a). This cooling owes to the pronounced upward longwave emission from ice clouds in the cloud canopy, which are optically opaque in the presence of such

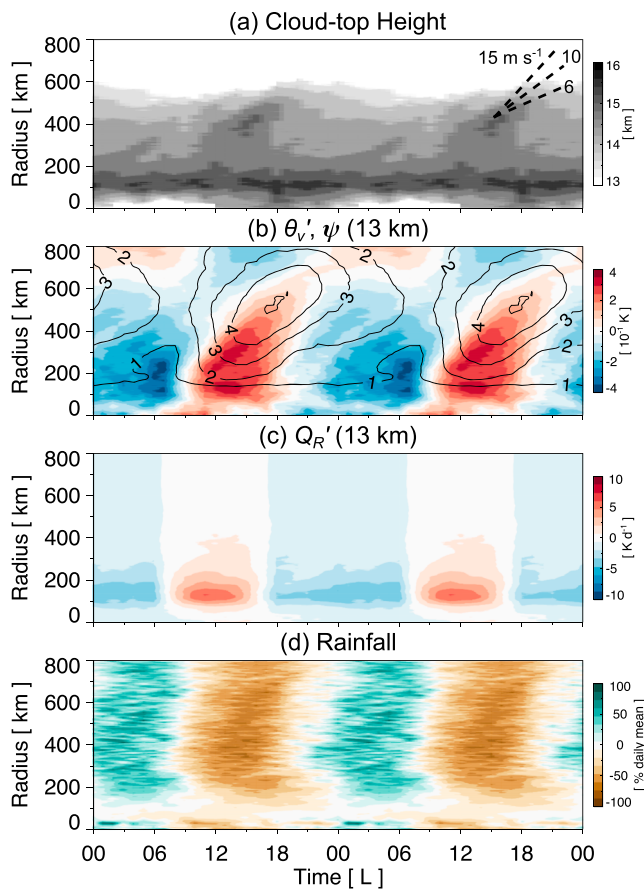


Figure 3. Time-radius sections of (a) cloud top height (km; the height at which q_t crosses the threshold 1 mg/kg); (b) virtual potential temperature departure from the daily and radial composite mean θ'_v (10^{-1} K) and ψ at 13 km (contours; 10^8 kg/s); (c) Q'_R at 13 km (daily mean removed; K/day); and (d) rainfall as percent of daily mean. The sloped lines in the legend of (a) indicate phase speeds of 6, 10, and 15 m/s.

homogenizing Q'_R virtually removed the upper-level transverse circulation response. Furthermore, Navarro et al. (2017) found that in an axisymmetric framework, the transverse circulation in the TC inner core adjusts rapidly to maintain first-order balance with a diurnally varying (unrectified sinusoidal) heat source. If instantaneous balance is assumed, then the response of w' to a change in Q'_R can be approximated from $w' = Q'_R(ds/dz)^{-1}$, where s is dry static energy (assumed to be constant). Estimating w' through this equation for radial averages over 100–300 km yields a midday maximum of ~ 40 mm/s at 12 km vertically, in first-order agreement with the w' maximum in Figure 2b, and that estimated from theory in an axisymmetric framework (30 mm/s; Navarro et al., 2017). The reason that the daytime peak in w' is ~ 1 km higher than that in Q'_R is unknown, though we speculate that it is caused by a lower-order diurnal change in latent heating at upper levels.

The response of clouds to the diurnal circulation change is depicted through time series of cloud liquid water path (LWP) and cloud IWP, that is, column-integrated nonprecipitating hydrometeors (Figure 2c). The corresponding time series of w' at 5 and 13 km are shown for comparison, which emphasize the opposite phasing of circulation at these levels. LWP exhibits a single nocturnal-early-morning peak (~ 02 – 08 L), which correlates nearly perfectly with w' at 5 km (Pearson correlation = 0.98). LWP therefore characterizes the behavior of the nocturnally enhanced deep convection. IWP exhibits two peaks: a nocturnal peak linked to the nocturnal convection and an afternoon peak. This afternoon peak coincides with the peak in w' at 13 km. This peak clearly cannot be explained by deep convection and is instead most likely caused by the peak in w' at 13 km caused by shortwave warming.

vigorous convection (Webster & Stephens, 1980). During daytime, warming due to shortwave absorption nearly perfectly offsets longwave cooling in most places. The important exception is the high, thick anvil clouds of the TC inner core, where direct shortwave absorption causes net Q'_R warming of ~ 4 K/day slightly beneath the level of maximum nocturnal cooling (the decomposition of Q'_R into longwave and shortwave at 12 L is provided as Figure S1). The diurnal-anomaly signal Q'_R averaged within the TC inner core further emphasizes the very top-heavy nature of this diurnal heating/cooling cycle (Figure 2b). These Q'_R patterns are consistent with the signatures of thick anvils previously reported (Powell et al., 2012; Webster & Stephens, 1980).

The top-heavy diurnal radiative heating-cooling cycle described above induces a top-heavy variation in temperature of $O(1$ K) in the TC inner core (e.g., Figure 7 of Navarro & Hakim, 2016 and Figure 4 of Ruppert & Hohenegger, 2018). The resulting change in static stability or lapse rate is the primary driver of the nocturnal invigoration of deep convection and rainfall (Liu & Moncrieff, 1998; Ruppert & Hohenegger, 2018; Xu & Randall, 1995). An additional process that augments this nocturnal invigoration is the differential radiative cooling between the TC inner core and surrounding environment, which promotes low-level convergence into the inner core at night (Gray & Jacobson, 1977; Nicholls, 2015; Ruppert & Hohenegger, 2018). The increase of convection and latent heating due to these combined processes explains the nocturnal enhancement of circulation in the low-midtroposphere to first order (Figures 2a and 2b; Navarro et al., 2017) and is extremely similar to the diurnal circulation variation of a nonrotating patch of deep convection (Ruppert & Hohenegger, 2018).

While the daytime increase of static stability caused by the strong upper-level shortwave warming stifles deep convection and rainfall during the daytime, the early-afternoon w' maximum in the upper troposphere can be interpreted as the thermally direct circulation response to this upper-level maximum in heating (Figures 2a and 2b). This warming maximizes in the TC inner core, where cloud optical thickness is the greatest. In a nonrotating framework, Ruppert and Hohenegger (2018) found that removing this localized upper-level Q'_R cycle by horizontally

To assess the robustness of these diurnal variations, the error bar for each variable is shown along the right ordinate in Figure 2c, calculated as the temporal standard deviation from the 25-day daily-averaged time series (i.e., prior to diurnal compositing). The diurnal cycle may be deemed statistically significant when its range exceeds the length of the error bar. By this measure, the diurnal cycles of both LWP and w' (at both height levels) are significant, while that of IWP is not. The larger error bar of IWP indicates that ice clouds are modulated by both the diurnal cycle and other (potentially stochastic) variability. Additional simulations may nevertheless provide further aid in assessing the robustness of these variations. To this end, the simulations R1-1500 (blue) and R1-2500 (red) are included in Figure 2c, composited for the same sample period (cf. Figure 1). The diurnal cycle of each variable is remarkably similar in each of these simulations. Specifically, each simulation is characterized by a composite-mean afternoon peak in IWP, which cannot be explained by deep convection, and is therefore most likely caused by the daytime radiative heating and subsequent increase in w' at 13 km.

Cloud top height is shown as a function of time and radius in Figures 3a and 3b to more clearly depict the transient nature of the daytime upper-level circulation signature and its manifestation in the TC cloud canopy. Cloud top height generally decreases from ~ 16 to ≤ 13 km from radii of 100–600 km (Figure 2a). A pronounced signal embedded within this mean pattern is a daytime expansion of high clouds: namely, clouds of ~ 14 – 15 -km height begin extending outward from the TC inner core shortly after 09 L. This expansion continues into progressively lower background cloud heights, reaching 600 km radially by ~ 19 L. This expansion is consistent in timing with the diurnal variation of canopy clouds in mature Atlantic hurricanes as seen in satellite measurements of infrared brightness temperature (Dunion et al., 2014).

The lifting of the circulation top exhibits a very similar outward radial progression, as indicated by increased values of ψ at 13 km (Figure 3b). The magnitude of the ψ change is the greatest from radii of ~ 300 – 700 km. The lifting of cloud top heights begins at virtually the same time as this increase ψ , that is, mid-late morning. Rainfall is diurnally suppressed at all radii throughout this period (Figure 3d), reaffirming the distinct behavior of boundary-layer rooted deep convection and the clouds and circulation at upper levels.

The beginning of this transient radial feature closely coincides with the onset of daytime radiative warming of the cloud canopy, as demonstrated by Q'_R at 13 km (Figure 3c). The buoyancy production caused by this radiative warming is illustrated through eddy virtual potential temperature θ'_v at 13 km (Figure 3b), calculated by subtracting the diurnal and radial average from the diurnal composite. θ'_v increases most dramatically between ~ 07 and 11 L and from ~ 100 – 300 km, that is, where the Q'_R signal is the greatest. While the diurnal signal in Q'_R weakens greatly beyond 300 km due to the decrease of cloud ice content (Figure 2a), the signal in θ'_v extends far beyond this radius.

Prior studies have shown that the circulation maintains approximate balance with the diurnal heat source at the innermost radii, where inertial stability is high, while inertia-gravity waves (IGWs) are excited at greater radii (Navarro & Hakim, 2016; Navarro et al., 2017; O'Neill et al., 2017). The threshold between these regimes is at ~ 200 km in the upper troposphere, sloping outward to >300 km in the lower troposphere (Navarro et al., 2017; O'Neill et al., 2017). The outward radial progression from ~ 200 km apparent in cloud top height, ψ , and θ'_v manifests at a rate of ~ 10 – 15 m/s in Figures 3a and 3b. The radial outflow at this level is ~ 4 – 6 m/s, and so advection cannot explain this outward progression. It is therefore likely explained by the IGW response to the diurnal heating. More specifically, Evans and Nolan (2018) showed that the radiative heating of the TC cloud canopy forces the IGW response, since it heats the TC at radii outside of the balanced regime of the TC, whereas deep convection primarily affects the balanced regime in the lower troposphere. Previous modeling studies noted horizontal IGW propagation rates of between 10 and 15 m/s in the upper troposphere, consistent with the propagation rate apparent in Figures 3a and 3b (Navarro & Hakim, 2016). There is little evidence of such propagation in surface rainfall (Figure 3d), suggesting that the upper-level IGW does not couple with precipitating convection in the lower-midtroposphere in this simulation.

We hypothesize that this upper-level IGW corresponds to the observed diurnal pulse of cloudiness in the TC canopy of mature Atlantic Hurricanes by Dunion et al. (2014). The propagation rate of 10–15 m/s apparent in Figure 3 is slightly faster than that in observations (~ 5 – 10 m/s). A potential cause for this discrepancy is the strong dryness due to artificially enhanced subsidence in the model domain outside of the convective core (not shown), which is a common characteristic of limited-area RCE simulations (Holloway et al., 2017). Strong dryness at outer radii could hypothetically impact the IGW propagation rate to the extent that it limits

the ability of the IGW to couple with clouds and rainfall and hence latent heating. This open question is left for future investigation.

4. Summary and Conclusions

This study has examined the diurnal cycle of TCs through cloud-permitting numerical simulations conducted in the rotating-RCE framework. We have sought to (1) identify the impact of the diurnal cycle on the timing of spontaneous tropical cyclogenesis and (2) explain the paradoxical diurnal behavior of anvil clouds in the cloud canopy of mature TCs, which peak (in height and areal coverage) in the afternoon despite the primary early-morning peak in rainfall. A miniature ensemble was conducted wherein TOA insolation was either varied diurnally or fixed to its daily mean. Within this ensemble, the diurnal cycle was found to have no apparent impact on the timing of spontaneous TC genesis. No past study has examined the nonlinear impact of the diurnal cycle on TC genesis in this manner, that is, keeping daily-mean insolation fixed as the control case.

Analysis of the diurnal cycle in a mature TC demonstrates that the afternoon maximum of anvil clouds and their height is caused by the thermally direct transverse circulation response to strong daytime shortwave warming in the TC cloud canopy. Since this shortwave warming and the resulting circulation response peaks near the top of the time-mean transverse circulation, it manifests in a lifting of the maximum height of the outflow and, in turn, both a lifting and invigoration of the anvil clouds within the TC cloud canopy. This lifting initially manifests in the inner core of the TC, that is, where clouds are optically the thickest, and hence where shortwave-cloud warming is the strongest. At radii beyond ~ 200 km, this effect propagates outward at 10–15 m/s in the form of an IGW excited by the upper-level radiative warming. We hypothesize that this IGW corresponds to the outward-propagating pulse of cloudiness observed in the cloud canopy of mature hurricanes by Dunion et al. (2014). We found slightly faster radial phase speeds compared to the observations, however. This discrepancy may owe to strong dryness outside of the TC inner core due to artificially enhanced subsidence in a limited-area model domain. Future studies should investigate this possibility.

The results of this study emphasize the measure to which the transverse circulation of TCs dramatically departs from its daily-averaged in-up-and-out structure. This departure owes its depth-dependent response to the out-of-phase diurnal cycles of latent heating and shortwave-cloud warming, which cause the overturning circulation at low–midlevels to peak overnight, and that in the upper troposphere to peak during daytime, respectively. These findings add to mounting evidence of such a two-layered diurnal evolution of overturning circulation in a range of organized deep convective systems, including in axisymmetric simulations (Navarro et al., 2017), nonrotating aggregated deep convection (Ruppert & Hohenegger, 2018), and the ITCZ (Ciesielski et al., 2018).

The afternoon increase of midlevel convergence associated with the afternoon circulation pattern suggests that TCs are more susceptible to the detrimental effects of dry-air entrainment, or ventilation, in the afternoon. The findings of this study also imply that the model prediction of the diurnally varying transverse circulation may be sensitive to the physical parameterizations of radiation and microphysics, as well as vertical grid spacing to the measure that it impacts the representation of the outflow, anvil clouds, and their radiative forcing. Future studies should be conducted to quantify these sensitivities.

References

- Bergman, J. W., & Salby, M. L. (1997). The role of cloud diurnal variations in the time-mean energy budget. *Journal of Climate*, *10*(5), 1114–1124. [https://doi.org/10.1175/1520-0442\(1997\)010<1114:TROCDV>2.0.CO;2](https://doi.org/10.1175/1520-0442(1997)010<1114:TROCDV>2.0.CO;2)
- Blake, E. S., & Zelinsky, D. A. (2018). National hurricane center tropical cyclone report: Hurricane harvey. Miami, FL. <https://doi.org/AL092017>
- Bowman, K. P., & Fowler, M. D. (2015). The diurnal cycle of precipitation in tropical cyclones. *Journal of Climate*, *28*(13), 5325–5334. <https://doi.org/10.1175/JCLI-D-14-00804.1>
- Bretherton, C. S., Blossey, P. N., & Khairoutdinov, M. (2005). An energy-balance analysis of deep convective self-aggregation above uniform SST. *Journal of the Atmospheric Sciences*, *62*(12), 4273–4292. <https://doi.org/10.1175/JAS3614.1>
- Chavas, D. R., Reed, K. A., & Knaff, J. A. (2017). Physical understanding of the tropical cyclone wind-pressure relationship. *Nature Communications*, *8*(1), 1360. <https://doi.org/10.1038/s41467-017-01546-9>
- Chen, S. S., & Houze, R. A. (1997). Diurnal variation and life-cycle of deep convective systems over the tropical Pacific warm pool. *Quarterly Journal of the Royal Meteorological Society*, *123*(538), 357–388. <https://doi.org/10.1002/qj.49712353806>

Acknowledgments

J. H. R. gratefully acknowledges funding for this research from the National Science Foundation (grant AGS-1524844) and Alexander von Humboldt Foundation/Stiftung. M. E. O. was primarily supported by the T. C. Chamberlin Postdoctoral Fellowship at the University of Chicago during this work. We thank Guido Cioni and two anonymous reviewers for their very constructive comments. We acknowledge Cathy Hohenegger and the Deutsches Klimarechenzentrum (DKRZ) for providing access to supercomputing resources. Model source code, start data, representative model output, and preprocessing and postprocessing scripts used in this study are archived by the Max Planck Institute for Meteorology and may be freely obtained with no restrictions from the online database at <https://pure.mpg.de/pubman/faces/HomePage.jsp>.

- Ciesielski, P. E., Johnson, R. H., Schubert, W. H., & Ruppert, J. H. (2018). Diurnal cycle of the ITCZ in DYNAMO. *Journal of Climate*, *31*(11), 4543–4562. <https://doi.org/10.1175/JCLI-D-17-0670.1>
- Clough, S. A., Shephard, M. W., Mlawer, E. J., Delamere, J. S., Iacono, M. J., Cady-Pereira, K., et al. (2005). Atmospheric radiative transfer modeling: A summary of the AER codes. *Journal of Quantitative Spectroscopy and Radiative Transfer*, *91*(2), 233–244. <https://doi.org/10.1016/j.jqsrt.2004.05.058>
- Cronin, T. W., Emanuel, K. A., & Molnar, P. (2015). Island precipitation enhancement and the diurnal cycle in radiative-convective equilibrium. *Quarterly Journal of the Royal Meteorological Society*, *141*(689), 1017–1034. <https://doi.org/10.1002/qj.2443>
- Dai, A. (2001). Global precipitation and thunderstorm frequencies. Part II: Diurnal variations. *Journal of Climate*, *14*, 1112–1128. [https://doi.org/10.1175/1520-0442\(2001\)014<1112:GPATFP>2.0.CO;2](https://doi.org/10.1175/1520-0442(2001)014<1112:GPATFP>2.0.CO;2)
- Davis, C. A. (2015). The formation of moist vortices and tropical cyclones in idealized simulations. *Journal of the Atmospheric Sciences*, *72*(9), 3499–3516. <https://doi.org/10.1175/JAS-D-15-0027.1>
- Dipankar, A., Stevens, B., Heinze, R., Moseley, C., Zängl, G., Giorgetta, M., & Brdar, S. (2015). Large eddy simulation using the general circulation model ICON. *Journal of Advances in Modeling Earth Systems*, *7*, 963–986. <https://doi.org/10.1002/2015MS000431>
- Dirmeyer, P. A., Cash, B. A., Kinter, J. L., Jung, T., Marx, L., Satoh, M., et al. (2012). Simulating the diurnal cycle of rainfall in global climate models: Resolution versus parameterization. *Climate Dynamics*, *39*(1–2), 399–418. <https://doi.org/10.1007/s00382-011-1127-9>
- Dunion, J. P., Thorncroft, C. D., & Velden, C. S. (2014). The tropical cyclone diurnal cycle of mature hurricanes. *Monthly Weather Review*, *142*(10), 3900–3919. <https://doi.org/10.1175/MWR-D-13-00191.1>
- Evans, R. C., & Nolan, D. S. (2018). Dynamical responses to diurnal heating in tropical cyclones as seen in a linear model. Extended Abstract for the 33rd Conference on Hurricanes and Tropical Meteorology.
- Gray, W. M., & Jacobson, R. W. (1977). Diurnal variation of deep cumulus convection. *Monthly Weather Review*, *105*, 1171–1188.
- Holloway, C. E., Wing, A. A., Bony, S., Muller, C., Masunaga, H., L'Ecuyer, T. S., et al. (2017). Observing convective aggregation. *Surveys in Geophysics*, *38*(6), 1199–1236. <https://doi.org/10.1007/s10712-017-9419-1>
- Houze, R. A. (1997). Stratiform precipitation in regions of convection: A meteorological paradox? *Bulletin of the American Meteorological Society*, *78*(10), 2179–2196. [https://doi.org/10.1175/1520-0477\(1997\)078<2179:SPIROC>2.0.CO;2](https://doi.org/10.1175/1520-0477(1997)078<2179:SPIROC>2.0.CO;2)
- Iacono, M. J., Delamere, J. S., Mlawer, E. J., Shephard, M. W., Clough, S. A., & Collins, W. D. (2008). Radiative forcing by long-lived greenhouse gases: Calculations with the AER radiative transfer models. *Journal of Geophysical Research*, *113*, D13103. <https://doi.org/10.1029/2008JD009944>
- Khairoutdinov, M., & Emanuel, K. (2013). Rotating radiative-convective equilibrium simulated by a cloud-resolving model. *Journal of Advances in Modeling Earth Systems*, *5*, 816–825. <https://doi.org/10.1002/2013MS000253>
- Kikuchi, K., & Wang, B. (2008). Diurnal precipitation regimes in the global tropics*. *Journal of Climate*, *21*(11), 2680–2696. <https://doi.org/10.1175/2007JCLI2051.1>
- Kimball, S. K. (2006). A modeling study of hurricane landfall in a dry environment. *Monthly Weather Review*, *134*(7), 1901–1918. <https://doi.org/10.1175/MWR3155.1>
- Kossin, J. P. (2002). Daily hurricane variability inferred from goes infrared imagery. *Monthly Weather Review*, *130*(9), 2260–2270. [https://doi.org/10.1175/1520-0493\(2002\)130<2260:DHVIFG>2.0.CO;2](https://doi.org/10.1175/1520-0493(2002)130<2260:DHVIFG>2.0.CO;2)
- Kraus, E. B. (1963). The diurnal precipitation change over the sea. *Journal of the Atmospheric Sciences*, *20*(6), 551–556. [https://doi.org/10.1175/1520-0469\(1963\)020<0551:TDPcot>2.0.CO;2](https://doi.org/10.1175/1520-0469(1963)020<0551:TDPcot>2.0.CO;2)
- Leppert, K. D., & Cecil, D. J. (2016). Tropical cyclone diurnal cycle as observed by TRMM. *Monthly Weather Review*, *144*(8), 2793–2808. <https://doi.org/10.1175/MWR-D-15-0358.1>
- Liu, C., & Moncrieff, M. W. (1998). A numerical study of the diurnal cycle of tropical oceanic convection. *Journal of the Atmospheric Sciences*, *55*(13), 2329–2344. [https://doi.org/10.1175/1520-0469\(1998\)055<2329:ANSOTD>2.0.CO;2](https://doi.org/10.1175/1520-0469(1998)055<2329:ANSOTD>2.0.CO;2)
- Mapes, B., Tulich, S., Lin, J., & Zuidema, P. (2006). The mesoscale convection life cycle: Building block or prototype for large-scale tropical waves? *Dynamics of Atmospheres and Oceans*, *42*(1–4), 3–29. <https://doi.org/10.1016/j.dynatmoce.2006.03.003>
- Melhauser, C., & Zhang, F. (2014). Diurnal radiation cycle impact on the pregenesis environment of Hurricane Karl (2010). *Journal of the Atmospheric Sciences*, *71*(4), 1241–1259. <https://doi.org/10.1175/JAS-D-13-0116.1>
- Mlawer, E. J., Taubman, S. J., Brown, P. D., Iacono, M. J., & Clough, S. A. (1997). Radiative transfer for inhomogeneous atmospheres: RRTM, a validated correlated-k model for the longwave. *Journal of Geophysical Research*, *102*(D14), 16663. <https://doi.org/10.1029/97JD00237>
- Navarro, E. L., & Hakim, G. J. (2016). Idealized numerical modeling of the diurnal cycle of tropical cyclones. *Journal of the Atmospheric Sciences*, *73*(10), 4189–4201. <https://doi.org/10.1175/JAS-D-15-0349.1>
- Navarro, E. L., Hakim, G. J., & Willoughby, H. E. (2017). Balanced response of an axisymmetric tropical cyclone to periodic diurnal heating. *Journal of the Atmospheric Sciences*, *74*(10), 3325–3337. <https://doi.org/10.1175/JAS-D-16-0279.1>
- Neale, R., & Slingo, J. (2003). The maritime continent and its role in the global climate: A GCM study. *Journal of Climate*, *16*(5), 834–848. [https://doi.org/10.1175/1520-0442\(2003\)016<0834:TMCAIR>2.0.CO;2](https://doi.org/10.1175/1520-0442(2003)016<0834:TMCAIR>2.0.CO;2)
- Nicholls, M. E. (2015). An investigation of how radiation may cause accelerated rates of tropical cyclogenesis and diurnal cycles of convective activity. *Atmospheric Chemistry and Physics Discussions*, *15*(5), 6125–6205. <https://doi.org/10.5194/acpd-15-6125-2015>
- Nolan, D. S., Zhang, C., & Chen, S.-h. (2007). Dynamics of the shallow meridional circulation around intertropical convergence zones. *Journal of the Atmospheric Sciences*, *64*(7), 2262–2285. <https://doi.org/10.1175/JAS3964.1>
- O'Neill, M. E., Perez-Betancourt, D., & Wing, A. A. (2017). Accessible environments for diurnal-period waves in simulated tropical cyclones. *Journal of the Atmospheric Sciences*, *74*(8), 2489–2502. <https://doi.org/10.1175/JAS-D-16-0294.1>
- Powell, S. W., Houze, R. A., Kumar, A., & McFarlane, S. A. (2012). Comparison of simulated and observed continental tropical anvil clouds and their radiative heating profiles. *Journal of the Atmospheric Sciences*, *69*(9), 2662–2681. <https://doi.org/10.1175/JAS-D-11-0251.1>
- Randall, D. A., Harshvardhan, & Dazlich, D. A. (1991). Diurnal variability of the hydrologic cycle in a general circulation model. *Journal of the Atmospheric Sciences*, *48*(1), 40–62. [https://doi.org/10.1175/1520-0469\(1991\)048<0040:DVOTHC>2.0.CO;2](https://doi.org/10.1175/1520-0469(1991)048<0040:DVOTHC>2.0.CO;2)
- Ruppert, J. H. (2016). Diurnal timescale feedbacks in the tropical cumulus regime. *Journal of Advances in Modeling Earth Systems*, *8*, 1483–1500. <https://doi.org/10.1002/2016MS000713>
- Ruppert, J. H., & Hohenegger, C. (2018). Diurnal circulation adjustment and organized deep convection. *Journal of Climate*, *31*(12), 4899–4916. <https://doi.org/10.1175/JCLI-D-17-0693.1>
- Ruppert, J. H., & Johnson, R. H. (2016). On the cumulus diurnal cycle over the tropical warm pool. *Journal of Advances in Modeling Earth Systems*, *8*, 669–690. <https://doi.org/10.1002/2015MS000610>
- Seifert, A., & Beheng, K. D. (2006). A two-moment cloud microphysics parameterization for mixed-phase clouds. Part 1: Model description. *Meteorology and Atmospheric Physics*, *92*(1–2), 45–66. <https://doi.org/10.1007/s00703-005-0112-4>
- Tang, B., & Emanuel, K. (2010). Midlevel ventilation's constraint on tropical cyclone intensity. *Journal of the Atmospheric Sciences*, *67*(6), 1817–1830. <https://doi.org/10.1175/2010JAS3318.1>

- Tang, X., & Zhang, F. (2016). Impacts of the diurnal radiation cycle on the formation, intensity, and structure of Hurricane Edouard (2014). *Journal of the Atmospheric Sciences*, *73*(7), 2871–2892. <https://doi.org/10.1175/JAS-D-15-0283.1>
- Webster, P. J., & Stephens, G. L. (1980). Tropical upper-tropospheric extended clouds: Inferences from winter MONEX. *Journal of the Atmospheric Sciences*, *37*(7), 1521–1541. <https://doi.org/10.1175/1520-0469-37.7.1521>
- Wing, A. A., Camargo, S. J., & Sobel, A. H. (2016). Role of radiative–convective feedbacks in spontaneous tropical cyclogenesis in idealized numerical simulations. *Journal of the Atmospheric Sciences*, *73*(7), 2633–2642. <https://doi.org/10.1175/JAS-D-15-0380.1>
- Wu, Q., & Ruan, Z. (2016). Diurnal variations of the areas and temperatures in tropical cyclone clouds. *Quarterly Journal of the Royal Meteorological Society*, *142*(700), 2788–2796. <https://doi.org/10.1002/qj.2868>
- Xu, K.-M., & Randall, D. A. (1995). Impact of interactive radiative transfer on the macroscopic behavior of cumulus ensembles. Part II: Mechanisms for cloud-radiation interactions. *Journal of the Atmospheric Sciences*, *52*(7), 800–817. [https://doi.org/10.1175/1520-0469\(1995\)052<0800:IOIRTO>2.0.CO;2](https://doi.org/10.1175/1520-0469(1995)052<0800:IOIRTO>2.0.CO;2)
- Yang, S., & Smith, E. A. (2006). Mechanisms for diurnal variability of global tropical rainfall observed from TRMM. *Journal of Climate*, *19*(20), 5190–5226. <https://doi.org/10.1175/JCLI3883.1>
- Yuan, J., & Houze, R. A. (2010). Global variability of mesoscale convective system anvil structure from a-train satellite data. *Journal of Climate*, *23*(21), 5864–5888. <https://doi.org/10.1175/2010JCLI3671.1>
- Zipser, E. J. (1969). The role of organized unsaturated convective downdrafts in the structure and rapid decay of an equatorial disturbance. *Journal of Applied Meteorology*, *8*(5), 799–814. [https://doi.org/10.1175/1520-0450\(1969\)008<0799:TROOUC>2.0.CO;2](https://doi.org/10.1175/1520-0450(1969)008<0799:TROOUC>2.0.CO;2)
- Zipser, E. J. (1977). Mesoscale and convective-scale downdrafts as distinct components of squall-line structure. *Monthly Weather Review*, *105*, 1568–1589.